



# Laboratory hydrogen laser-plasma and white-dwarf stars line shapes

Christian G. Parigger

University of Tennessee Space Institute

411 B. H. Goethert Parkway

Tullahoma, TN 37388

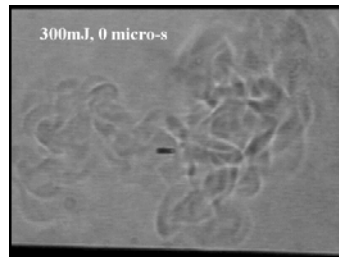


# Overview

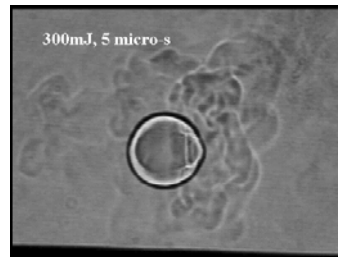
- Laser plasma fundamentals
- Stellar astrophysics spectra
- Optical breakdown in laboratory air
- Atomic hydrogen spectra:  $H_{\alpha}$  and  $H_{\beta}$
- Abel inverted atomic spectra
- Molecular CN spectra
- Abel inverted molecular spectra
- Atomic and molecular superposition spectra
- Nano-particle laser-induced plasma
- Conclusions



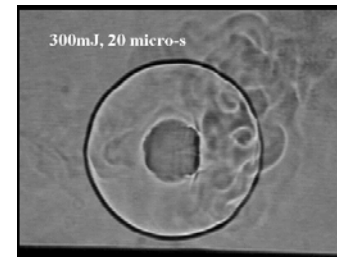
# Laser plasma shadowgraphs



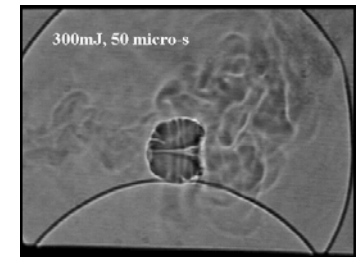
**Air Breakdown  
Shadowgraphs**



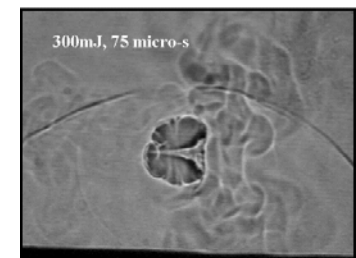
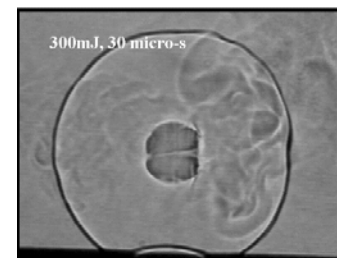
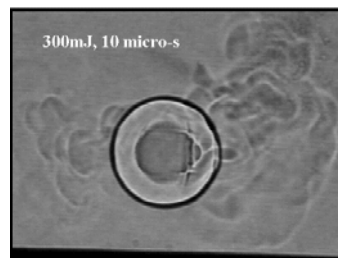
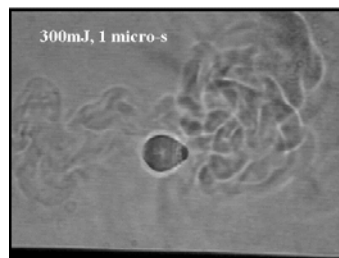
**Air Breakdown  
Shadowgraphs**



**Air Breakdown  
Shadowgraphs**



**Air Breakdown  
Shadowgraphs**



Temperature and density distribution at center, or at the “plasma kernel”; self-absorption? Energy/pulse: 300 mJ, 4 ns pulses; image size: 36 x48 mm; Double images showing fluid phenomena;

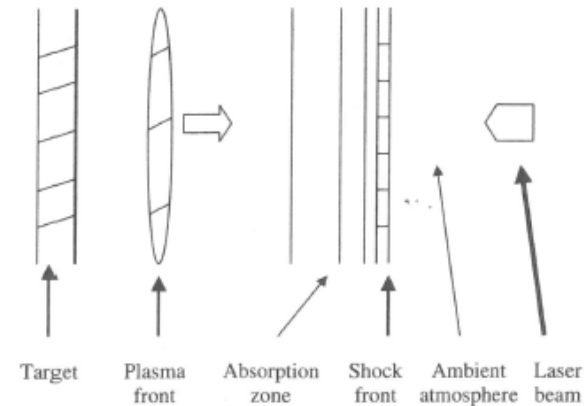
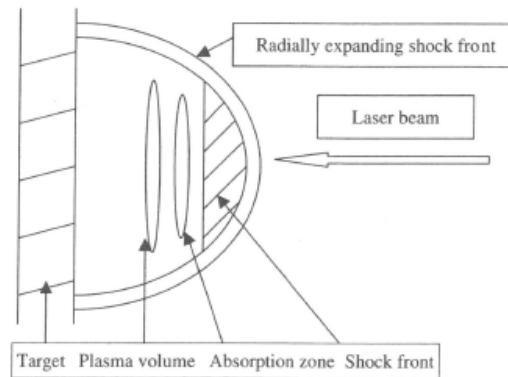
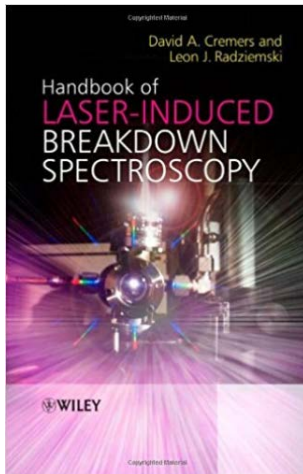
- Laser-induced expansion;
- Atomic spectra, molecular spectra;
- Equilibrium consideration in plasma kernel;
- Chemical imaging using molecular spectra;

**Visualization of Laser-Induced-Plasma,**  
**C. Parigger et al. OSA 1996;**  
<http://view.utsi.edu/cparigger/osa96/index.html>



# Laser plasma fundamentals

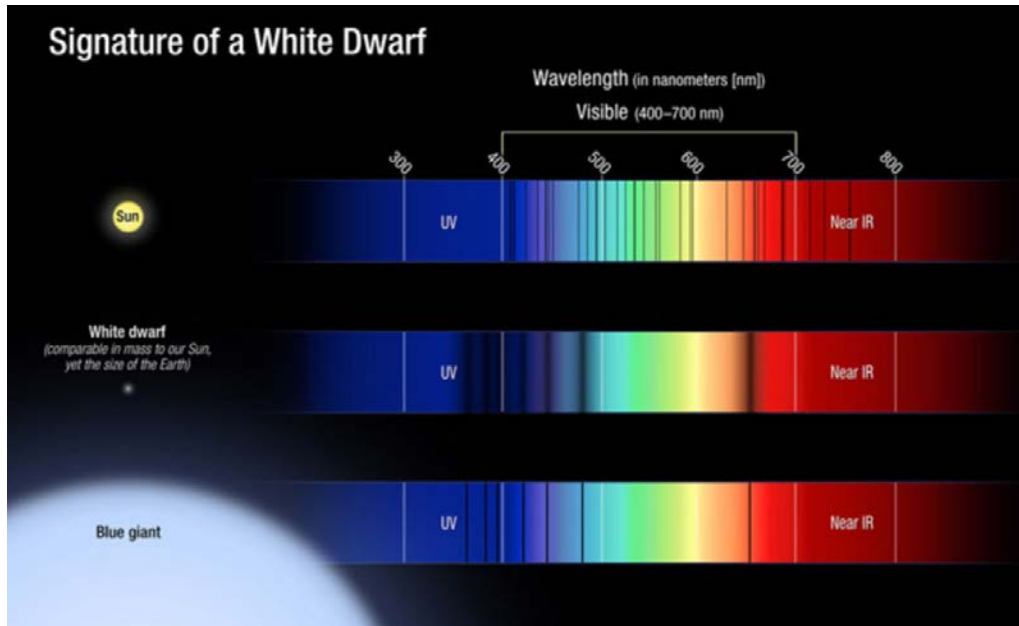
Post ns breakdown phenomena: plasma front, absorption front, shock front



- Laser-supported combustion (LCD) for low, above threshold irradiance: energy deposited behind shock + plasma radiation moves absorption front towards laser;
- Laser-supported detonation (LSD) for higher irradiances, the shock front heats gas leading to absorption;
- Laser-supported radiation (LSR) for highest irradiances, the radiation from the plasma heats atmosphere, absorption zone is coupled to plasma front;



# Stellar astrophysical spectra



Is it possible to measure laboratory micro-plasma, measurements, and analysis to apply in astrophysical studies?

Will time-resolved spectroscopy make it possible to measure accurate atomic and molecular spectra at high temperatures?

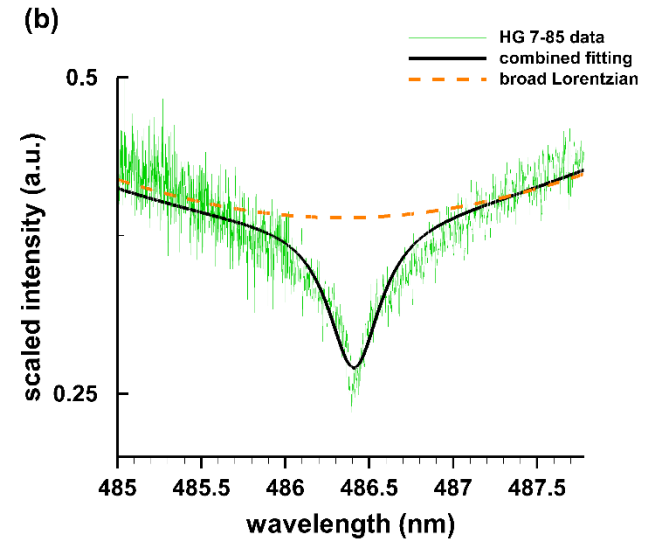
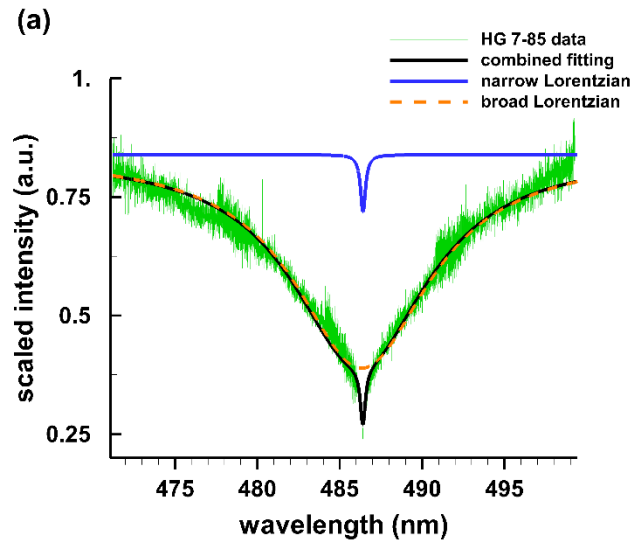
Atomic processes in plasma, Laser-induced breakdown spectroscopy?  
Sirius B: 26 kK, Procyon B: 7.9 kK

Measurement of emission spectra?

<http://dev.montrealwhitedwarfdatabase.org/tables-and-charts.html>



# Hyades cluster WD HG 7-85

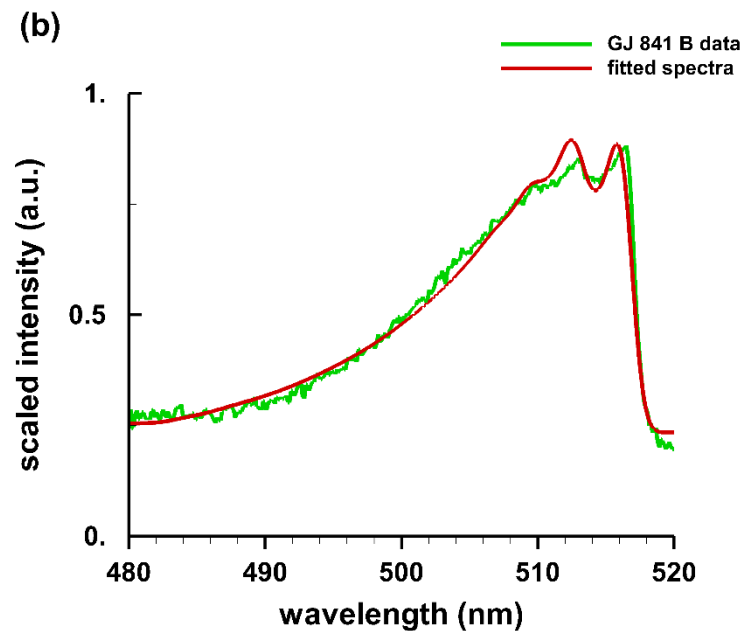
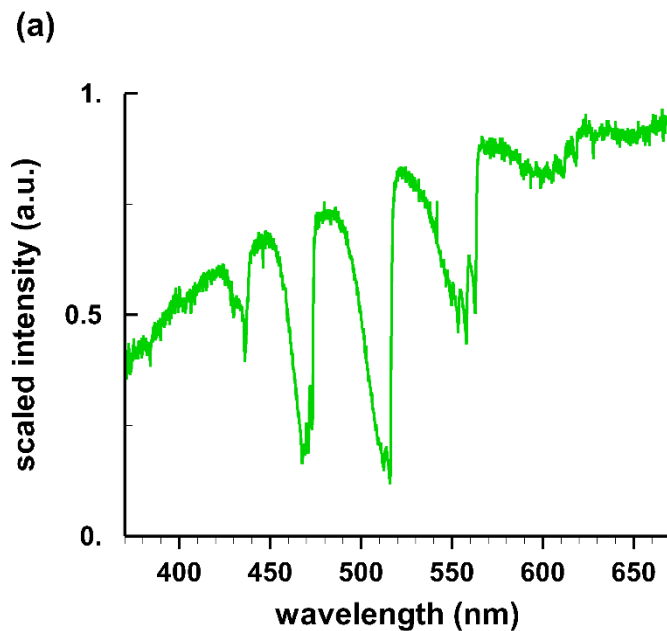


Hyades cluster white dwarf HG 7-85, recorded with a resolving-power 40,000 Echelle-spectrometer. (a) H expanded region, (b) H center portion.

Center  $\lambda\lambda$ : 486.22 nm, redshift: 0.08 nm; Grav. redshift: 44.3 km/s (0.072 nm)



# C<sub>2</sub> Swan spectra modeling of WD spectra

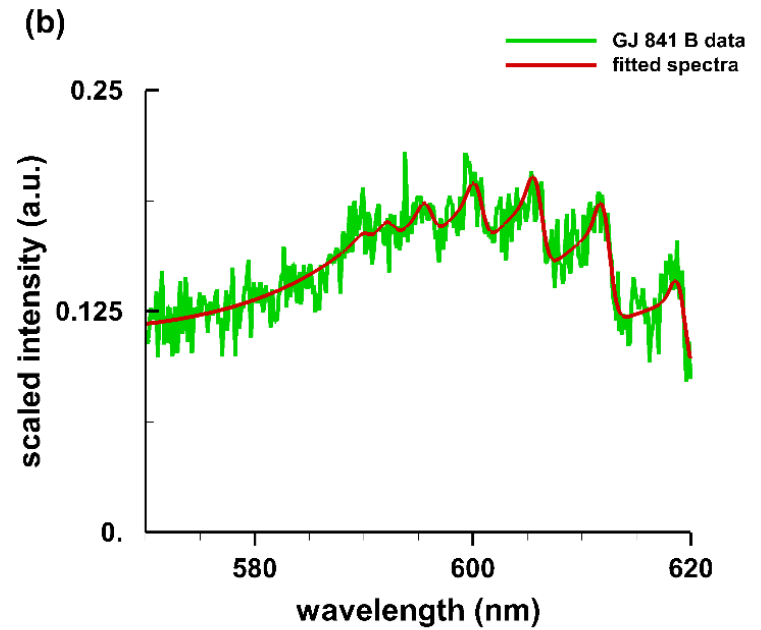
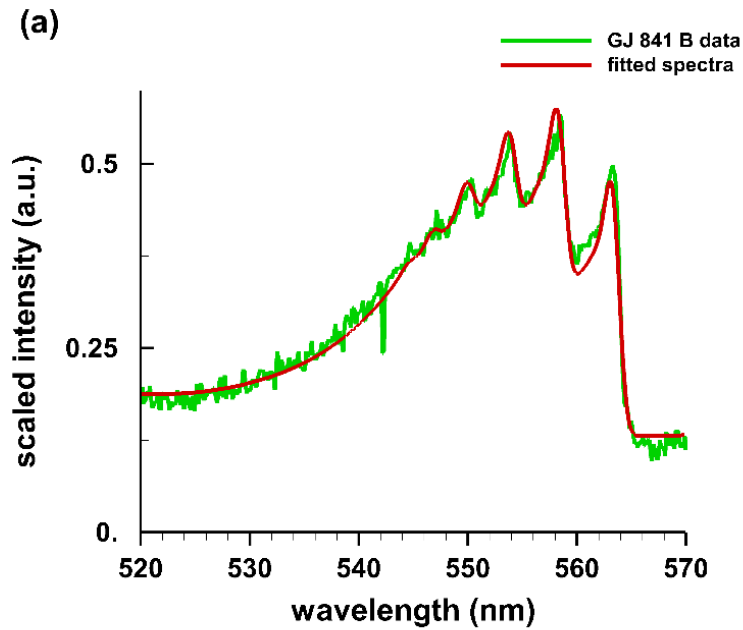


White dwarf GJ 841 B. (a) C<sub>2</sub> Swan absorption spectrum. (b)  $\Delta v = 0$ ,  
 $T = 7.1$  kK,  $\delta\lambda = 1.8$  nm.

C.G. Parigger et al., *Atoms* 6 (2018) 36



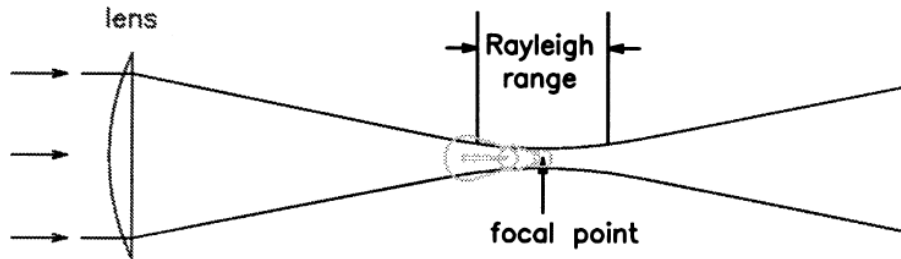
# C<sub>2</sub> Swan spectra, contd.



(a)  $\Delta v = -1$ ,  $T = 4.5$  kK,  $\delta\lambda = 1.5$  nm, (b)  $\Delta v = -2$ :  $T = 4.2$  kK,  $\delta\lambda = 1.5$  nm.



# Laser plasma focal volume



Chen, Lewis, Parigger,  
JQSRT 67, 91-103 (2000)

- (a) just below threshold
- (b) higher than threshold
- (c) much higher than threshold

$$X_R = \frac{\pi \omega_0^2}{\lambda}$$

$$T \propto I_L^{1/(\beta + 4)},$$

$$V \propto I_L^{4/(\beta + 4)},$$

$$\beta = 1.6$$

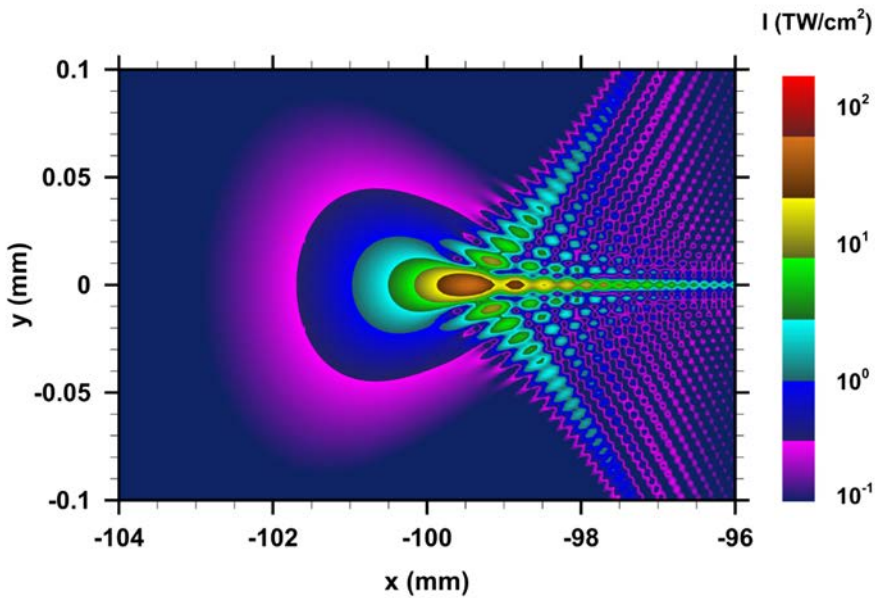
Table 1  
Irradiance dependant plasma temperature and propagation speed

$I_L$ (GW/cm <sup>2</sup> )	$T$ (K)	$V$ (km/s)
1.0	104,500	10.0
2.5	123,000	19.0
10.0	158,000	51.0
15.0	169,500	69.0
20.0	178,400	85.0
30.0	191,800	114.0

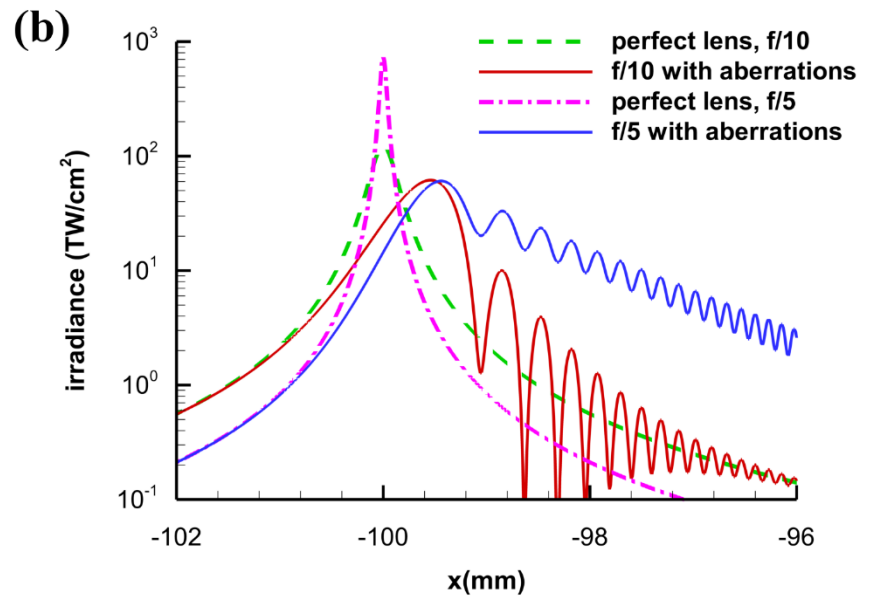


# Focal volume distributions

Results for 800 mJ, 6 ns Gaussian beam (Quintel Q-smart 850);  $2w_0 = \left(\frac{4\lambda}{\pi}\right)\left(\frac{F}{D}\right)$



f/5 focusing, Thorlab LA4545

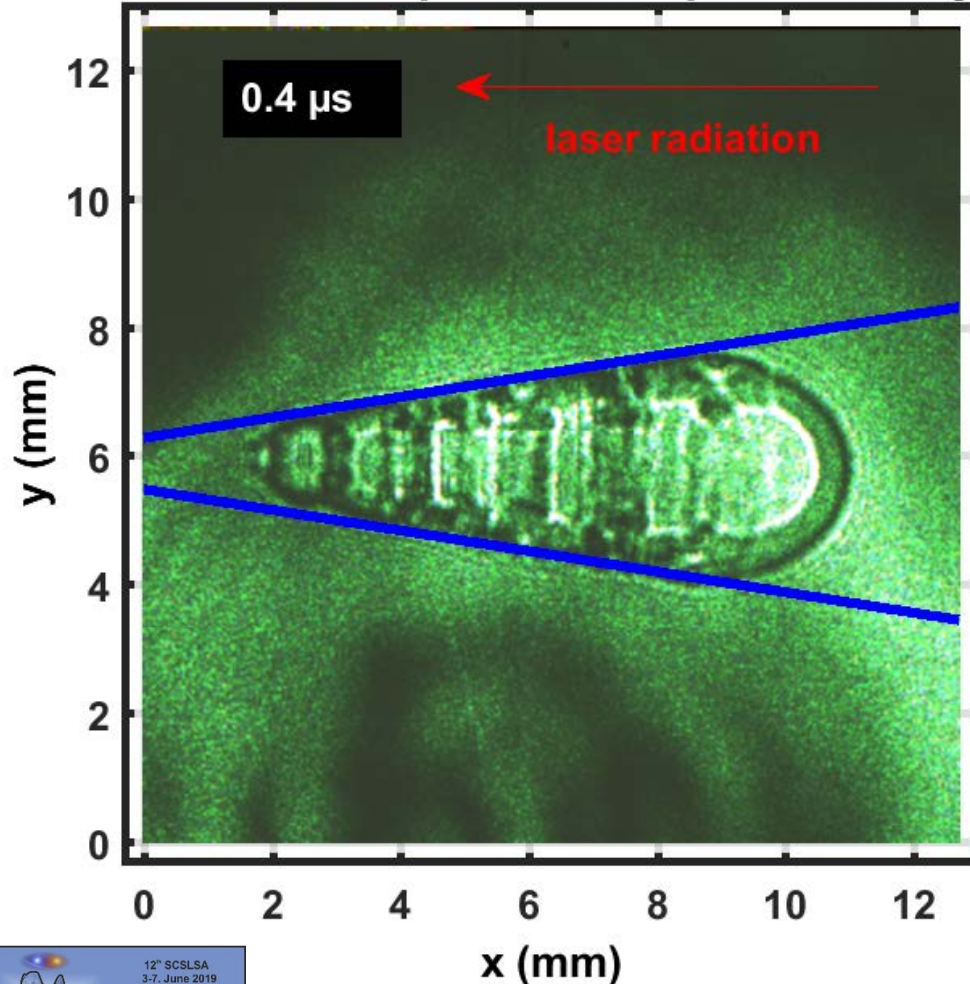


On-axis irradiance distributions

Parigger, Helstern, Gautam, IRAMP 8(1), 2017

# Optical breakdown in air

Laser-driven plasma: 0.4  $\mu\text{s}$  time delay



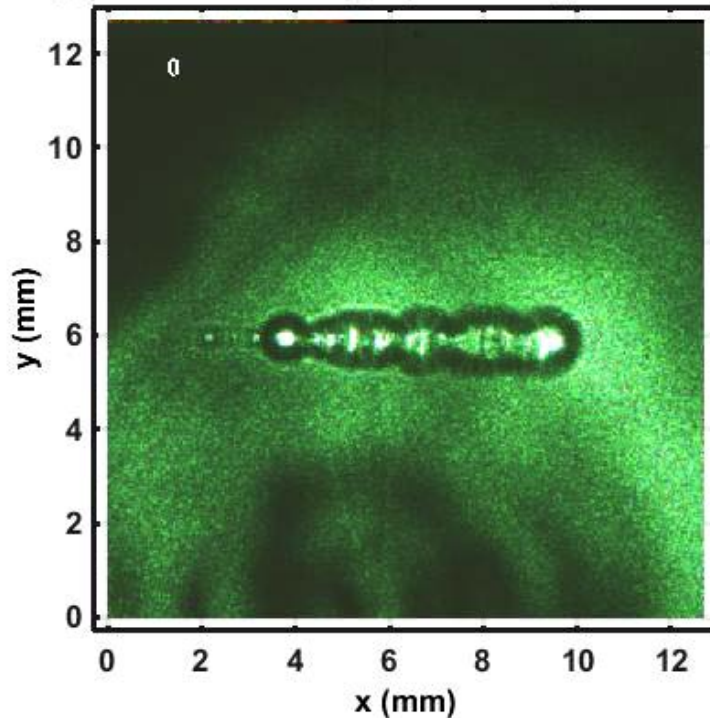
The shock wave maximum expands vertically in excess of Mach 6 ( $\sim 2$  km/s), and horizontally in excess of Mach 40 ( $\sim 14$  km/s) for a time delay of 0.4  $\mu\text{s}$ . Higher speeds are measured for shorter time delays from generation of the laser plasma. The blue lines indicate a cone and the significant, measured horizontal speed.

Gautam, Helstern, Drake, Parigger, IRAMP 7, 35-41 (2016).

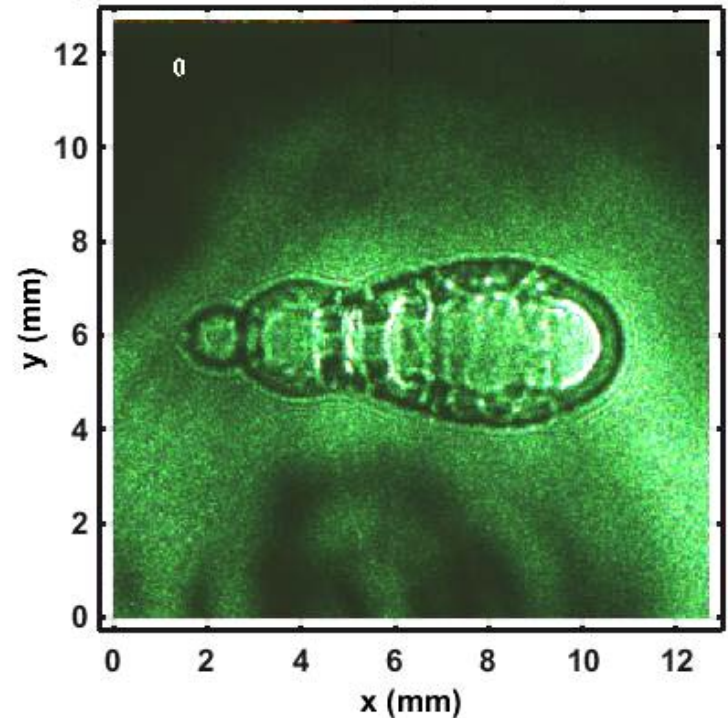


# Optical breakdown in air videos

Laser-plasma shadowgraph: 0.05  $\mu\text{s}$  time delay,

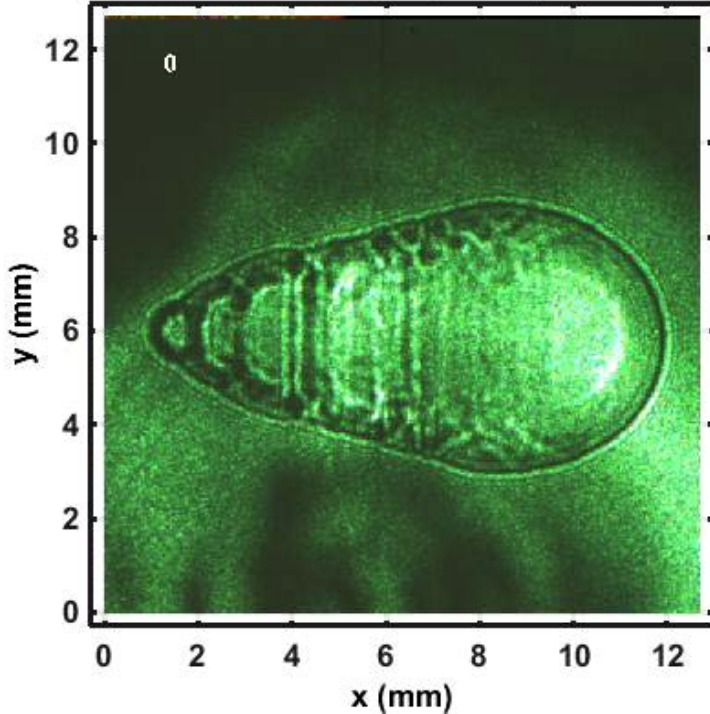


Laser-plasma shadowgraph: 0.4  $\mu\text{s}$  time delay, ai

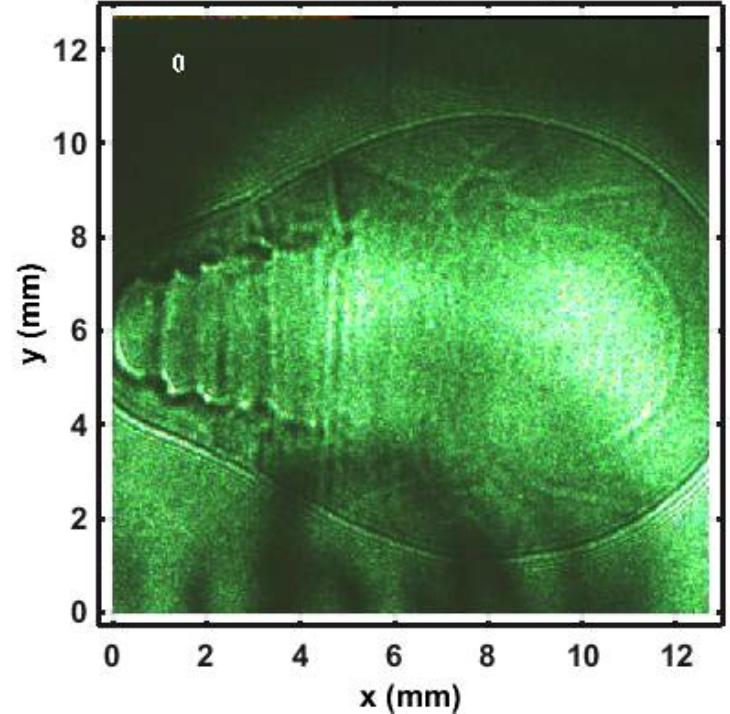


# Optical breakdown in air, contd.

Laser-plasma shadowgraph: 1  $\mu$ s time delay, air



Laser-plasma shadowgraph: 3  $\mu$ s time delay, air



**Taylor Sedov:**  $R(\tau) = (E/\rho \tau^2)^{1/5}$

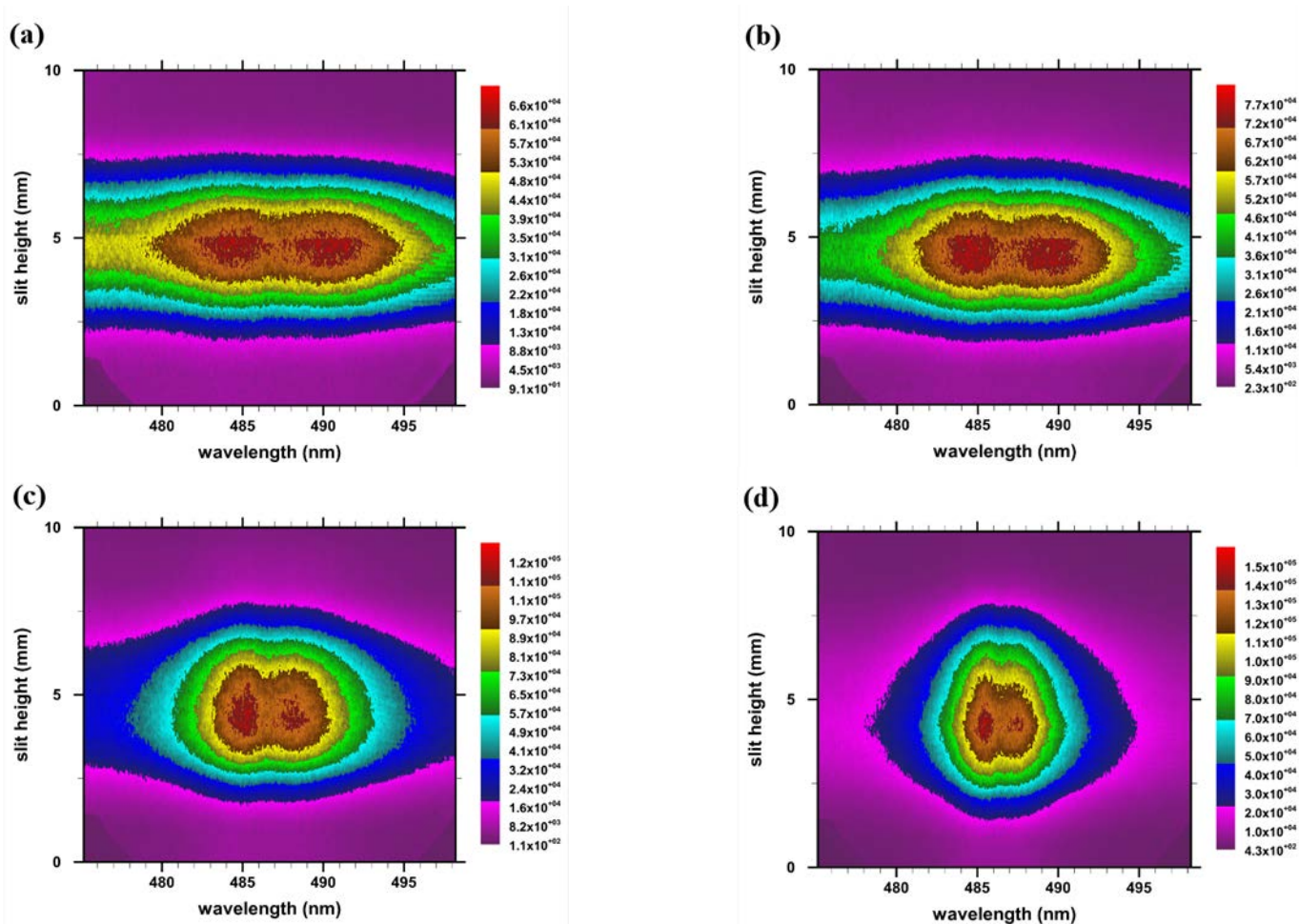
$E = 150 \text{ mJ}$ ,  $\tau = 0.4 \mu\text{s}$ ,  $\rho_{\text{Air}} = 1.2 \text{ kg/m}^3$ ,  $R_{\text{Air}}(0.4 \mu\text{s}) = 1.8 \text{ mm}$

$E = 150 \text{ mJ}$ ,  $\tau = 0.4 \mu\text{s}$ ,  $\rho_{\text{Hyd}} = 0.09 \text{ kg/m}^3$ ,  $R_{\text{Hyd}}(0.4 \mu\text{s}) = 3.1 \text{ mm}$

sound velocity ratio:  
hydrogen/air  $\approx 3.8$



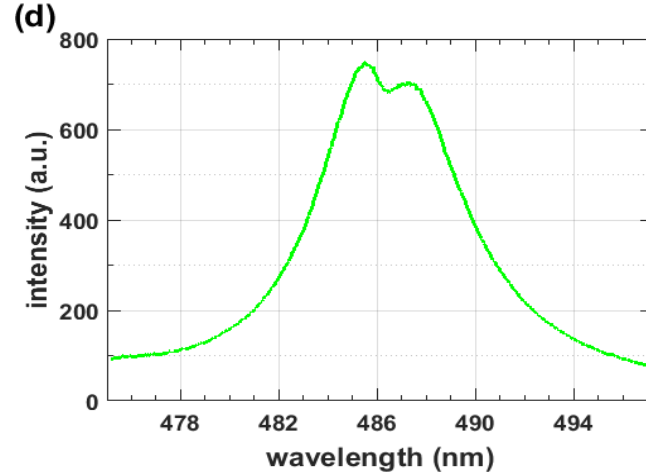
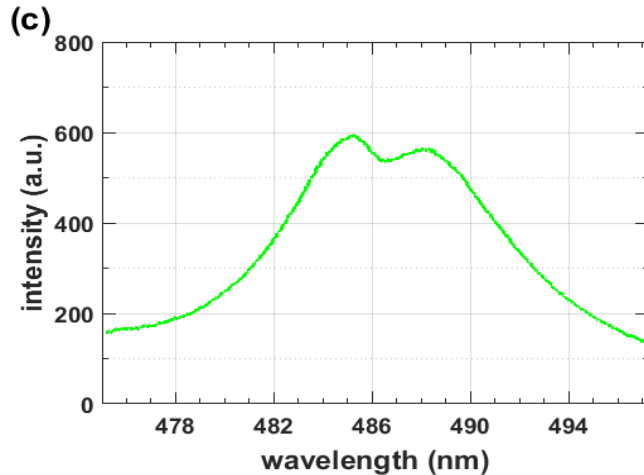
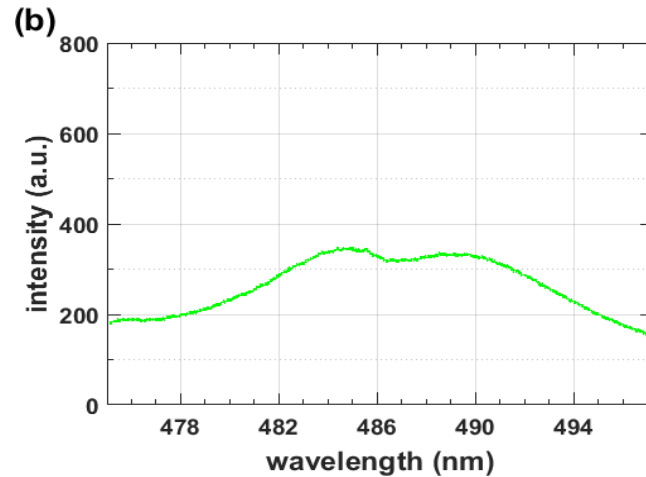
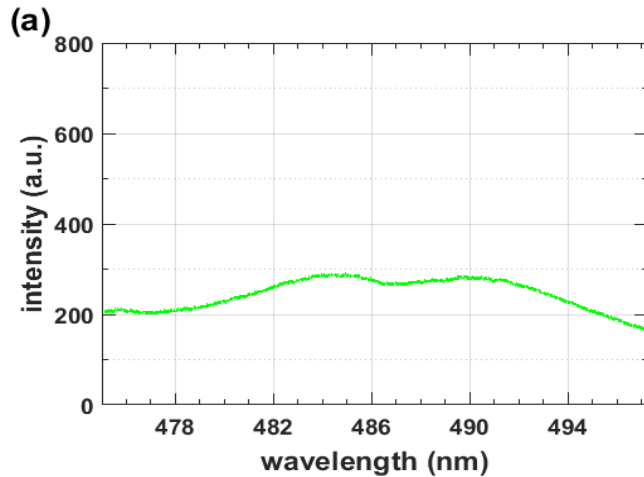
# Atomic spectra: H $\beta$



Measured H $\beta$  spectra. Gate width: 5 ns, time delay (a) 50 ns, (b) 75 ns, (c) 150 ns, and (d) 275 ns after optical breakdown in hydrogen gas at a pressure of  $0.76 \times 10^5$  Pa (11 psi)



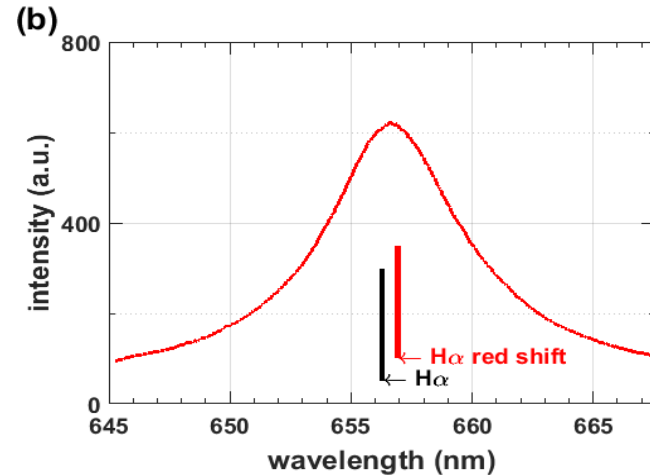
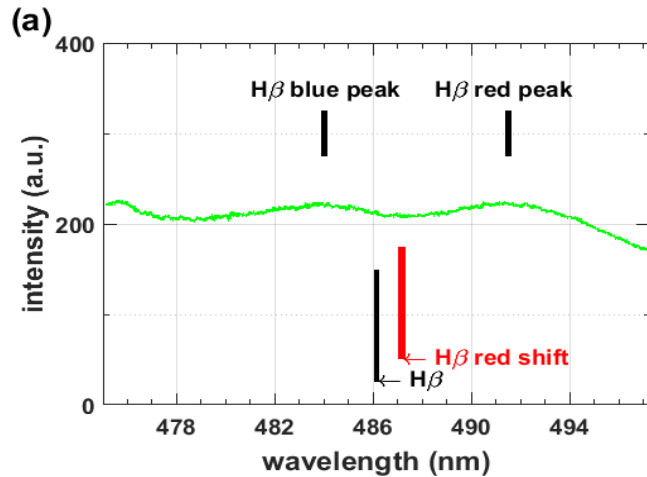
# Atomic spectra: $H_{\beta}$ , contd.



Average spectra of  $H_{\beta}$ . Gate width: 5 ns, time delay (a) 50 ns, (b) 75 ns, (c) 150 ns, and (d) 275 ns for a hydrogen gas at a pressure of  $0.76 \times 10^5$  Pa (11 psi)



# Atomic spectra: $H_\alpha$ and $H_\beta$



Average (a)  $H_\beta$  and (b)  $H_\alpha$  line shapes. Gate width: 5 ns, time delay 25 ns.  
 $H_2$  at  $0.76 \times 10^5$  Pa (11 psi)

$$\Delta\delta_{ds}[\text{nm}] = 0.14 \left( \frac{N_e[\text{cm}^{-3}]}{10^{17}} \right)^{0.67 \pm 0.03}$$

$$\Delta\delta_{\text{shift}}[\text{nm}] = 0.055 \left( \frac{N_e[\text{cm}^{-3}]}{10^{17}} \right)^{0.97 \pm 0.03}$$

$$\Delta w_{H_\beta}[\text{nm}] = 4.5 \left( \frac{N_e[\text{cm}^{-3}]}{10^{17}} \right)^{0.71 \pm 0.03}$$

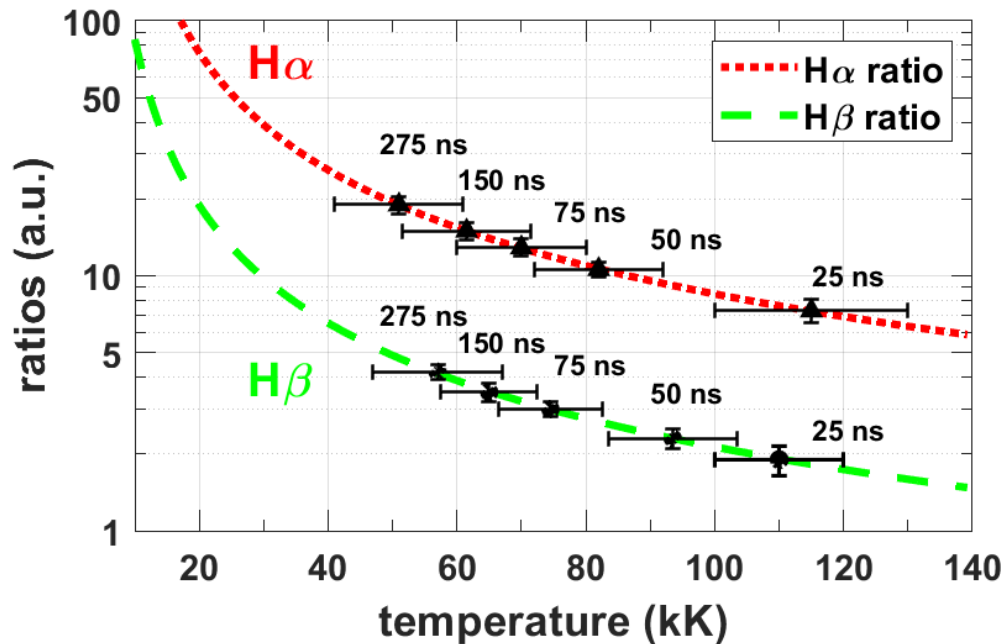
$$\Delta w_{H_\alpha}[\text{nm}] = 1.3 \left( \frac{N_e[\text{cm}^{-3}]}{10^{17}} \right)^{0.64 \pm 0.03}$$

$$\Delta w_{H_\beta} \sim 32 \times \Delta\delta_{ds}$$

$$\Delta\lambda_{ps}[\text{nm}] = 1.3 \left( \frac{N_e[\text{cm}^{-3}]}{10^{17}} \right)^{0.61 \pm 0.03}$$

Comment:  $H_\beta$  shift for astrophysical spectra

# Atomic spectra: H $\alpha$ and H $\beta$ , contd.



## Boltzmann plot:

$$T_e \text{ (eV)} = 1 / \ln [0.46 / (H_\beta / H_\alpha)]^{1.5}$$

## Comment on Doppler width:

$$\Delta\lambda_{1/2}^D = 7.16 \times 10^{-7} \lambda \sqrt{T/M}$$

$$R = \lambda / \Delta\lambda \sim 4 \times 10^3 \text{ } (\Delta\lambda \sim 0.1 \text{ nm})$$

$$\Delta\lambda_{1/2}^D / \Delta\lambda = 0.09 \sqrt{T[\text{kK}] / M}$$

$$T=64 \text{ kK}, M=1: \Delta\lambda_{1/2}^D / \Delta\lambda = 0.72$$

$$\Delta\lambda_{1/2}^D = 72 \text{ pm}$$

$$\Delta\lambda_V \approx \Delta\lambda_L / 2 + \sqrt{(\Delta\lambda_L / 2)^2 + \Delta\lambda_G^2}$$

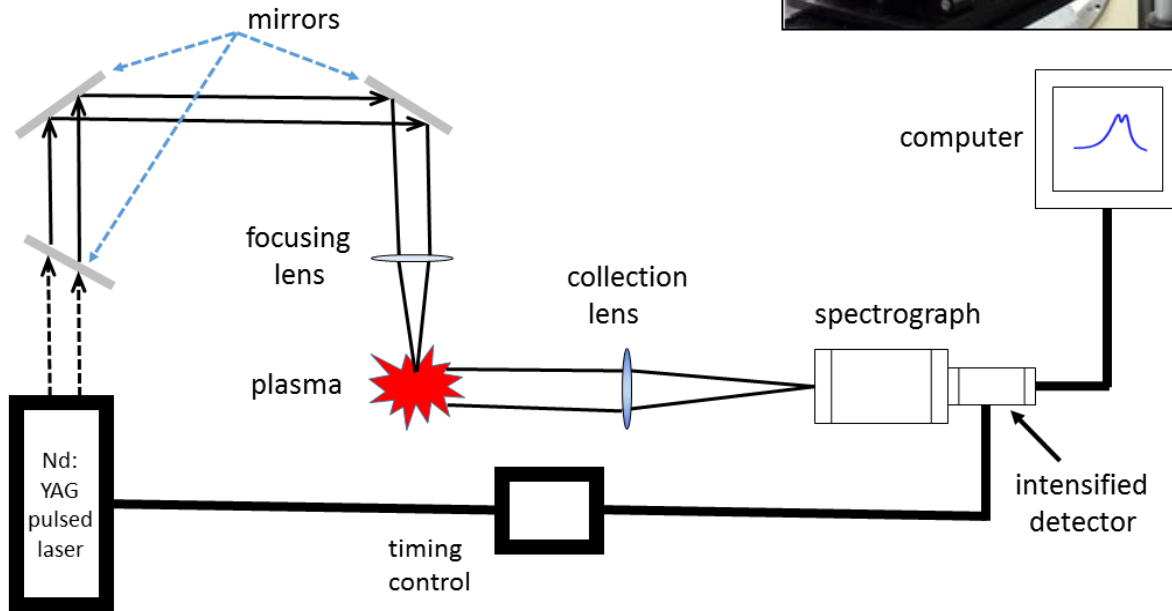
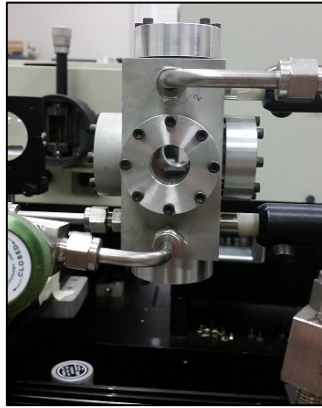
$$\Delta\lambda_V \sim 0.535 \Delta\lambda_L + \sqrt{0.217 \Delta\lambda_L^2 + \Delta\lambda_G^2}$$

Computed H $\alpha$  and H $\beta$  line to 10-nm continuum ratios. Time delays:  
25 ns, 50 ns, 75 ns, 150 ns, and 275 ns from optical breakdown using  
150 mJ, 6 ns laser pulses at 1064 nm in  $0.76 \times 10^5$  Pa (11 psi)

Parigger, Helstern, Drake, Gautam, IRAMP 8(2), 2017



# Experimental arrangement: Cell



Especially, thanks to David Surmick and Ghaneshwar Gautam!



# Self-absorption

**Absorption**  $A_{\text{total}} = \int (1 - e^{-k(\nu)l}) d\nu$

N. Omenetto et al., SA 30B (1975) 335;

COG: I.B. Gornushkin et al. SAB 54 (1999) 491

**Transmission**  $T(l, \nu) = e^{-k(\nu)l}$

Radiative transfer, Boltzmann integro-diff. equation

T. Holstein, PR 72 (1947) 1212;

Escape factor: F.E. Irons, JQSRT 22 (1979) 1

## Transmission of flame through flame

for  $k(\nu)l \ll 1$ : optically thin, absorption  $\sim k(\nu)l$

for  $k(\nu)l \gg 1$ :  $T = 2 - (2 - \sqrt{2}) = \sqrt{2}$ ;  $A = 2 - \sqrt{2}$

R. Ladenburg, F. Reiche, AdP 347 (1913) 181

T. Fujimoto, Plasma Spectroscopy, Clarendon, Oxford 2004

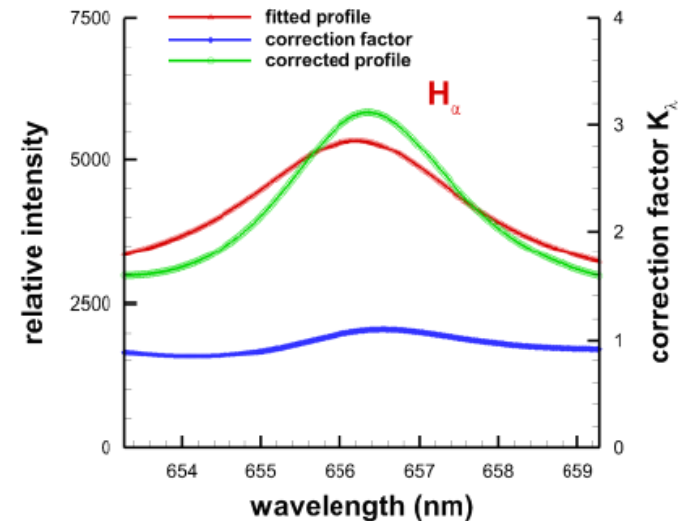
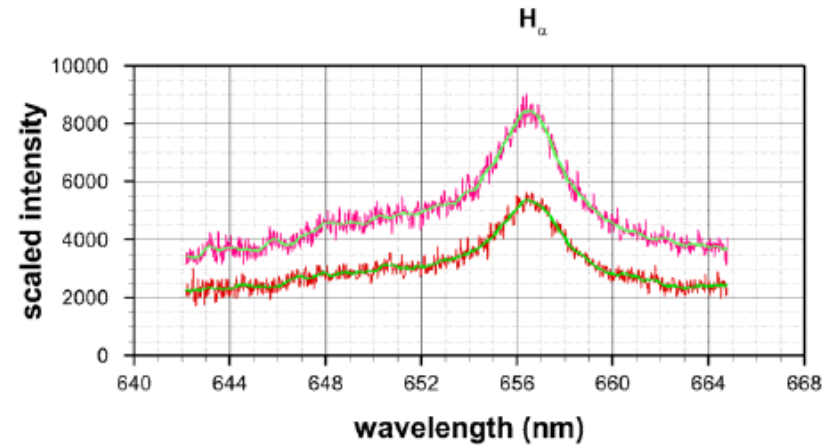
## Doubling mirror for optically thin plasma

Correction factor; self-absorption factor;

Electron density  $> 0.1 \text{ amg}$  self-absorption

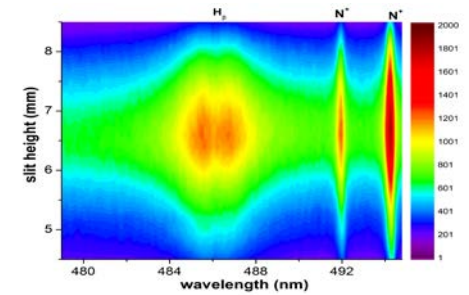
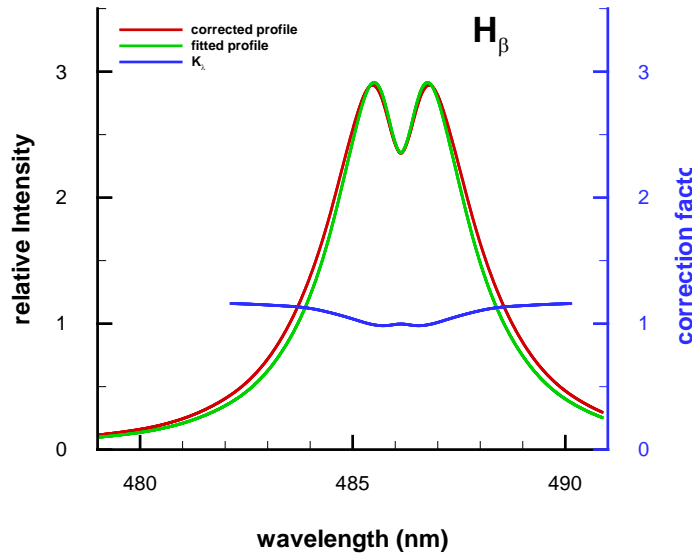
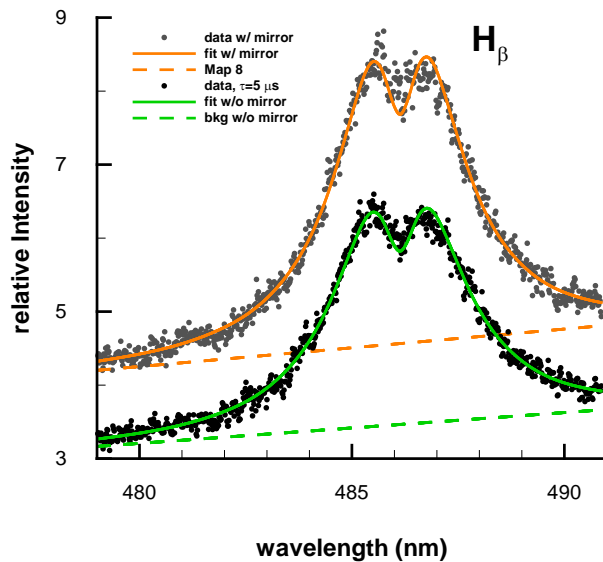
800 ns time delay: minimal self-absorption in SATP air plasma.

H-Y Moon et al., SAB 64 (2009) 702



# Hydrogen $\beta$ results: Air

## Laser-induced breakdown in air



5  $\mu$ s time delay,  $0.73 \times 10^{17} \text{ cm}^{-3}$  and  $0.69 \times 10^{17} \text{ cm}^{-3}$  without and with mirror, respectively. Insignificant self-absorption.  $K_\lambda = \log\{y\} / (y - 1)$ , with  $y = (R_\lambda - 1) / (R_C - 1)$ .

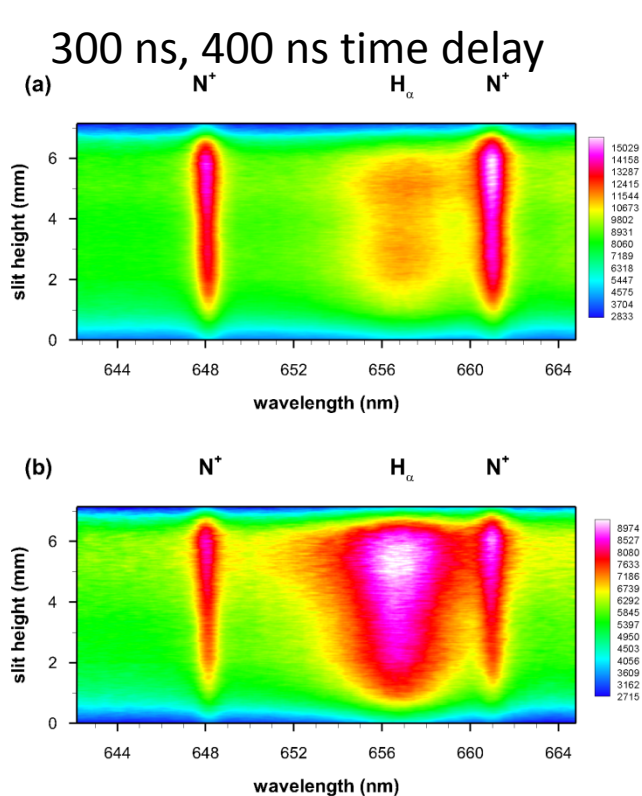
$$N_{e,\beta} [\text{m}^{-3}] = \left[ \frac{\Delta\lambda [\text{nm}]}{4.8} \right]^{1.46808} \times 10^{17}$$

$$\log N_{e,\beta} [\text{cm}^{-3}] = 16.661 + 1.416 \log \Delta\lambda_{ps} [\text{nm}] .$$

G.Gautam et al., JQSRT 170 (216) 189

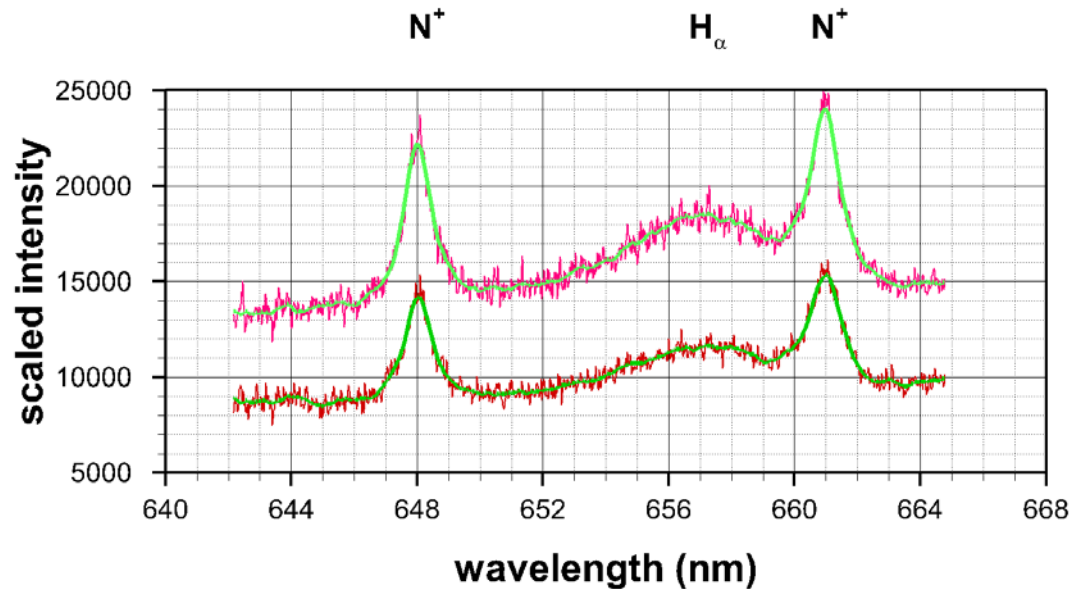


# Hydrogen $\alpha$ results: Air



The  $H_\alpha$  line is red-shifted from 656.28 nm, the  $N^+$  lines are only slightly shifted from 648.21 nm and 661.06 nm.

300 ns time delay

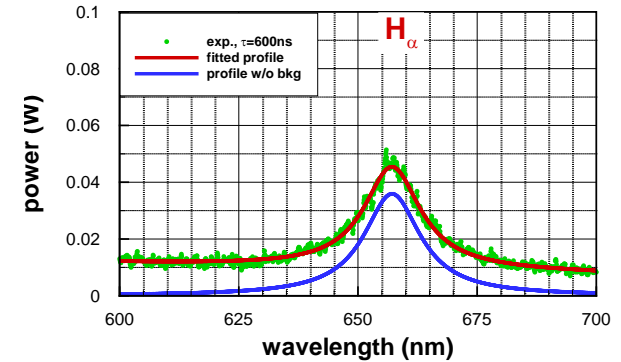
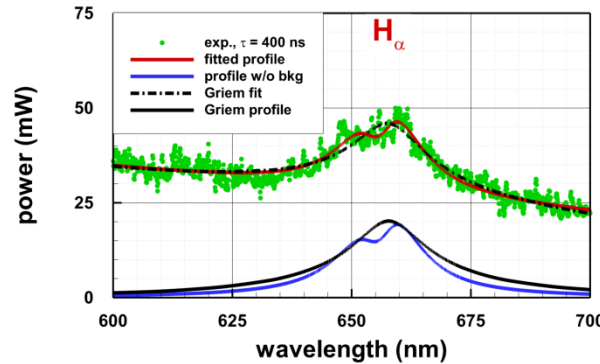
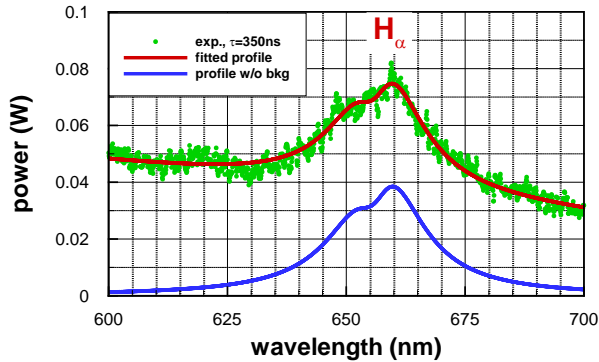


The electron density of  $14$  to  $20 \times 10^{17} \text{ cm}^{-3}$  determined from the  $H_\alpha$  line is higher than  $12$  to  $13 \times 10^{17} \text{ cm}^{-3}$  obtained from  $N^+$  for the 300 ns time delays. Therefore,  $H_\alpha$  shows self-absorption for delays of 300 ns; however, the level of self-absorption is insignificant for delays of 800 ns after optical breakdown.



# Hydrogen $\alpha$ spectra

Laser-induced breakdown of ice in air – collaboration with Ashraf M EL Sherbini in Cairo

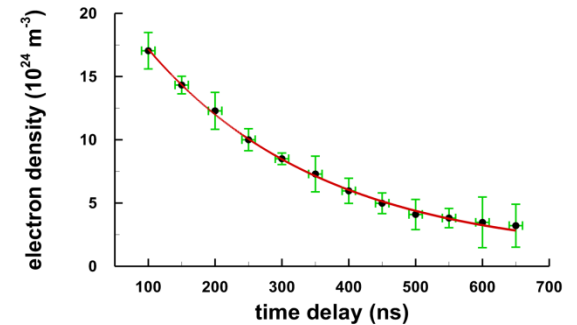
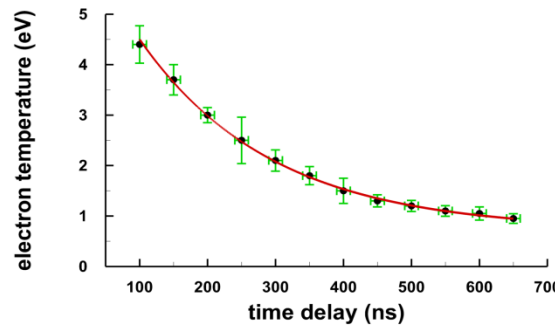


$\Delta\tau = 350$  ns (left) and  $\Delta\tau = 600$  ns (right).  $\Delta\lambda_S$  values of  $23 \pm 4$  nm and  $13 \pm 3$  nm for the time delays of 350 ns and 600 ns.  $N_e : 0.7 \times 10^{19} \text{ cm}^{-3}$  and  $0.3 \times 10^{19} \text{ cm}^{-3}$ . Red shifts  $\delta$  values are  $3.2 \pm 0.3$  nm and  $0.9 \pm 0.2$  nm,  $N_e : 0.8 \times 10^{19} \text{ cm}^{-3}$  and  $0.2 \times 10^{19} \text{ cm}^{-3}$ . Middle image shows comparison with Griem-data fit.

$N_e \approx 9 \times 10^{17} \lambda [\epsilon_\lambda^{ff}(T_e/E)^{1/2}]^{1/2}$   
Absolute emission coefficient!

$$\Delta\lambda_S [\text{nm}] = 5.68 \left[ \frac{N_e}{10^{24}} \right]^{0.64 \pm 0.03}$$

$$\delta [\text{nm}] = 0.543 \left[ \frac{N_e}{10^{24}} \right]^{0.97 \pm 0.03}$$

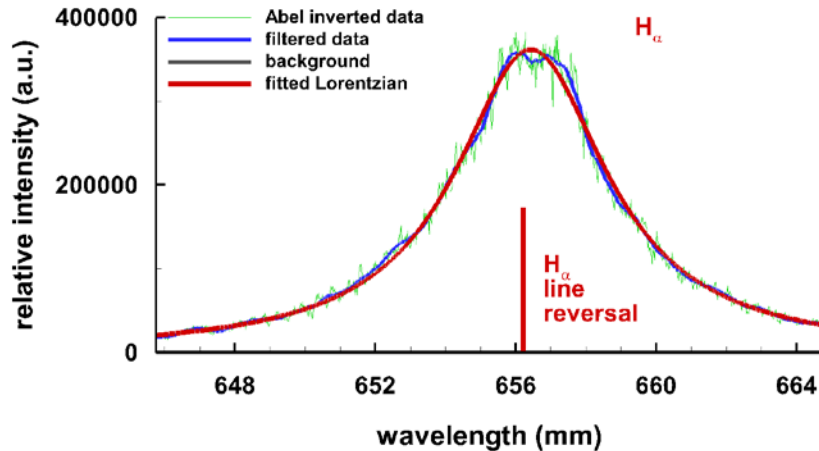


C.G. Parigger et al., OL 40 (2015) 3436

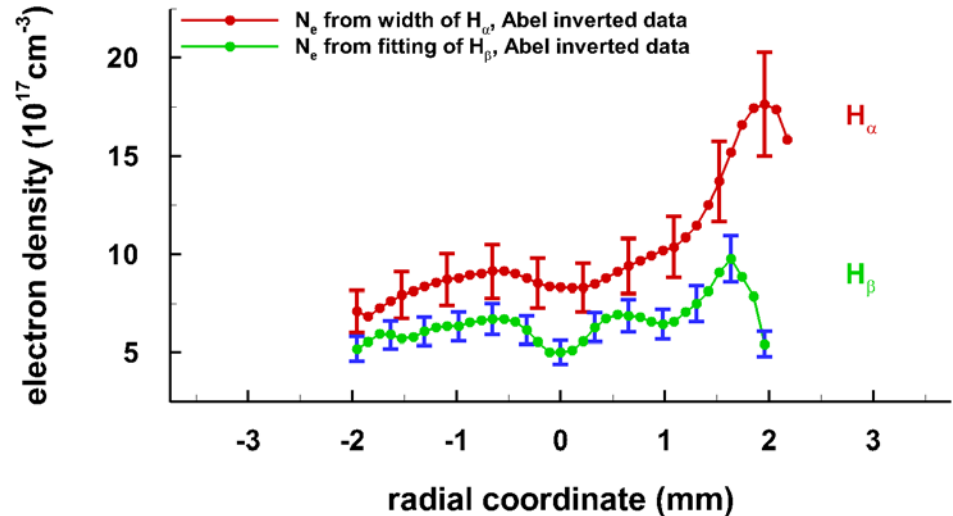




# H $\alpha$ and H $\beta$ : Abel inversion



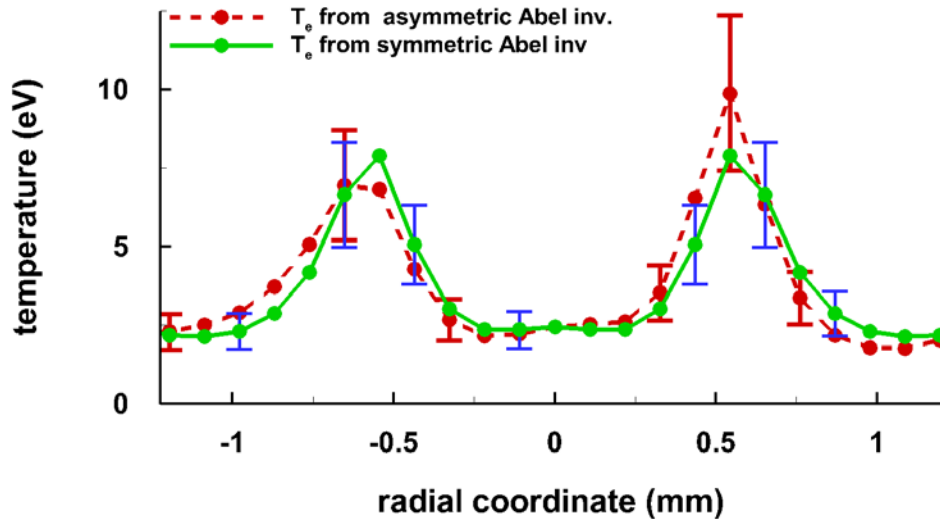
$N_e = 8.4 \times 10^{17} \text{ cm}^{-3}$ , UHP  
hydrogen gas (810 Torr),  
 $\tau = 0.15 \mu\text{s}$ .



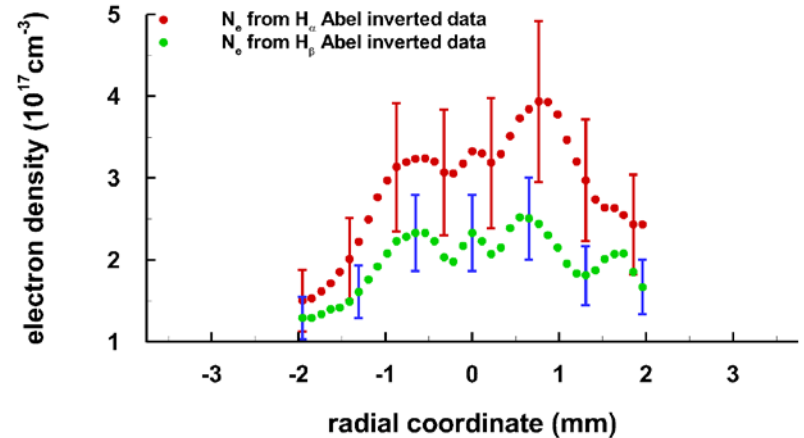
$N_e$  across the plasma from fitting  
Abel-inverted H $\alpha$  and H $\beta$  line profiles.



# H $_{\alpha}$ , H $_{\beta}$ and H $_{\gamma}$ : Abel inversion



T $_e$  from Boltzmann plots,  $\tau = 0.40 \mu\text{s}$ .



N $_e$  variation,  $\tau = 0.40 \mu\text{s}$ . N $_e$  is almost symmetric in the -1 to +1 mm range.

Adiabatic expansion  $T_1/T_2 = (N_1/N_2)^{2/3}$   
for  $T_1/T_2 = 2$ ,  $N_1 = 2.8 N_2$

T $_{\text{max}}$  expands at  $(1/[5/3])^{1/2}$ , see  
Mulser&Bauer, High Power Laser-Matter  
Interaction, Springer, Berlin, 2010

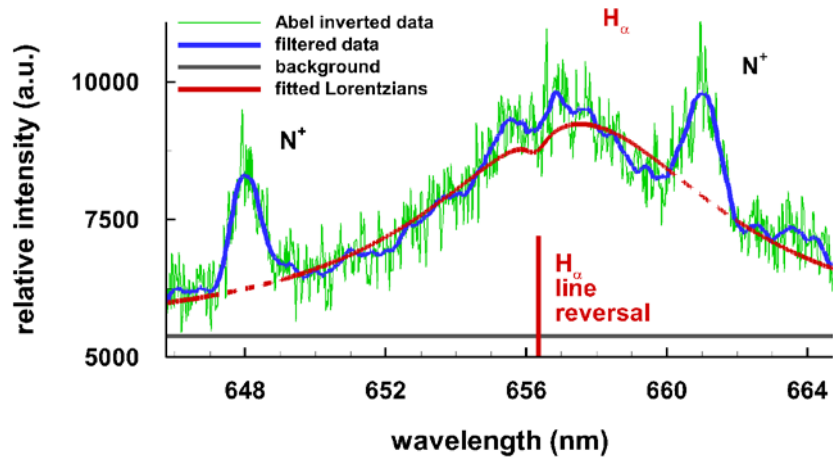
Keldysh parameter:  $\gamma = \frac{100}{\lambda(\mu\text{m})} \sqrt{\frac{E(\text{eV})\tau(\text{ns})}{\varphi(\text{J}/\text{cm}^2)}}$

E=13.6 eV,  $\tau=6 \text{ ns}$ ,  $\varphi = 85 \text{ J}/\text{cm}^2$  (850 mJ in 1 mm $^2$ ,  
 $\lambda=1 \mu\text{m}$ )

$\gamma = 100 \gg 1$  multiple photon absorption,  
no tunnel ionization

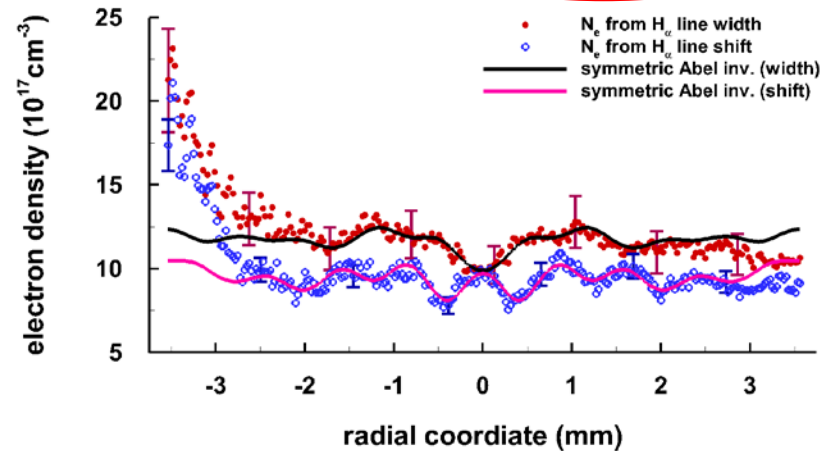
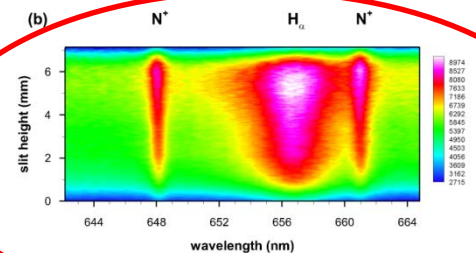
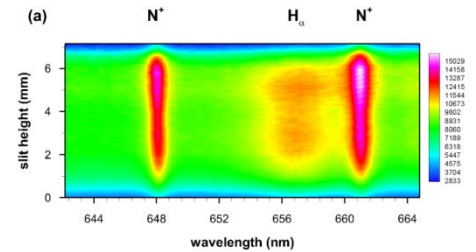


# Air breakdown: Abel inversion



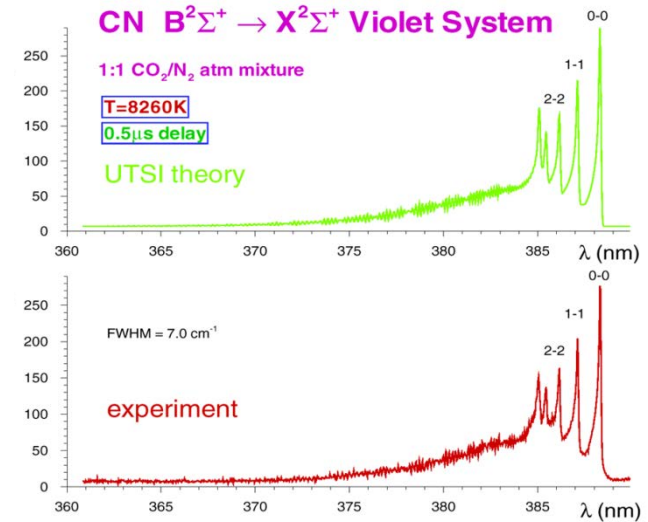
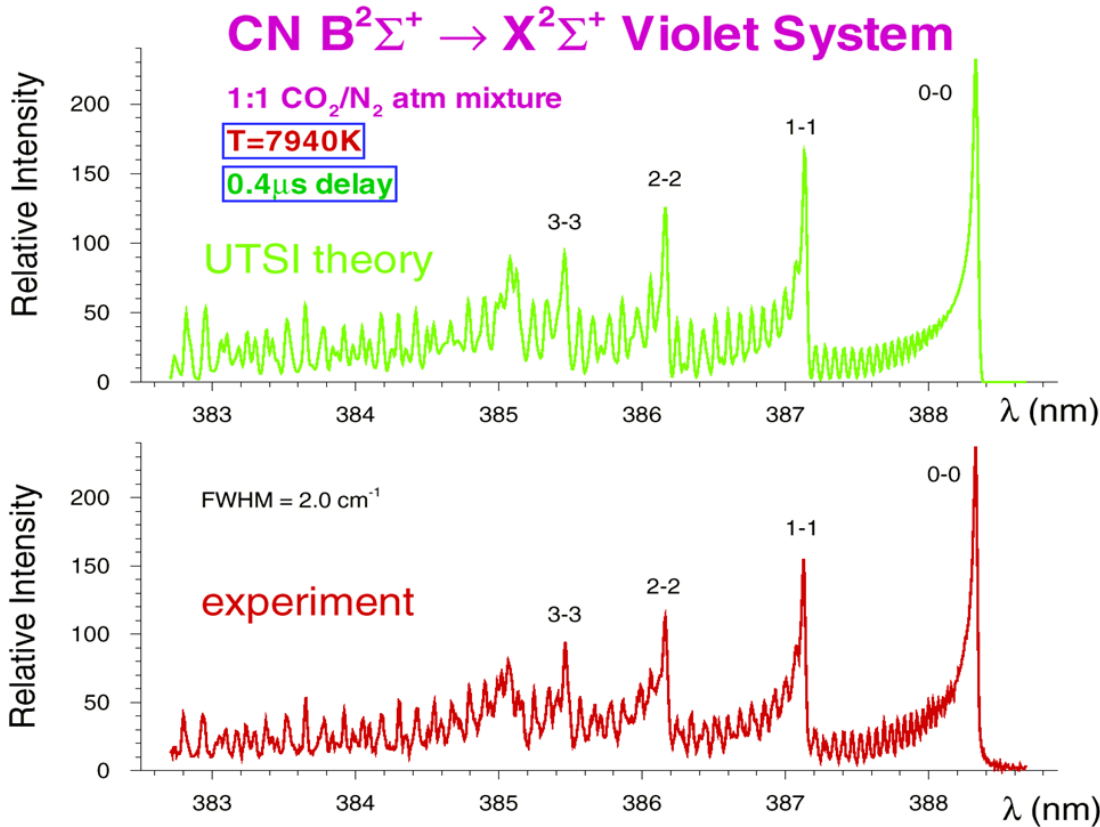
SATP air,  $N_e = 20 \times 10^{17} \text{ cm}^{-3}$ ,  $\tau = 0.40 \mu\text{s}$ .

Parigger, Surmick, Gautam,  
2017 J. Phys.: Conf. Ser. **810** 012012



$N_e$  variation from fitting Abel-inverted spectra

# CN molecular spectra



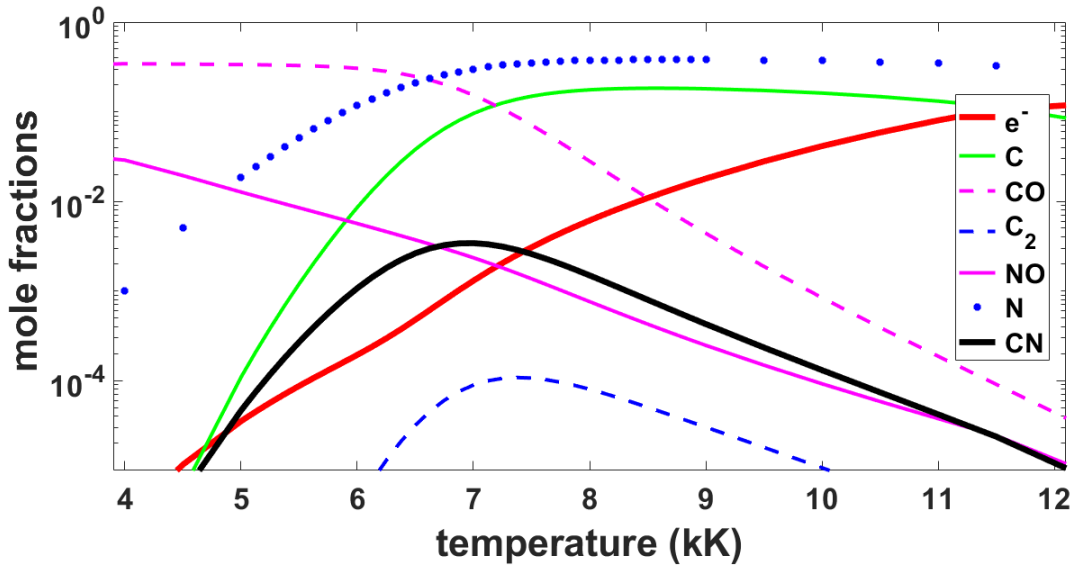
Used 35 ps laser radiation,  
 Actually,  $3 \times 35$  ps in 1 ns

**CN Spectrum for  $\Delta v = 0$ , resolution  $\sim 0.04$  nm**

Hornkohl, Parigger, Lewis, JQSRT **46**, 405 (1991)



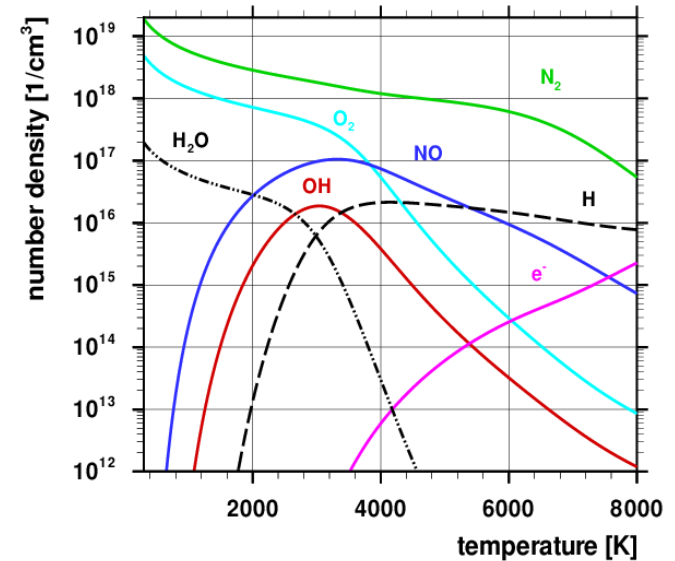
# CN molecular spectra



**Computed CN mole fraction versus temperature.**

In chemical equilibrium, CN shows a maximum near 7 kK for the 1:1 atmospheric  $CO_2:N_2$  mixture. Computed with CEA-code.

CN fractions in air are about  $500 \times$  lower than that for the mixture.



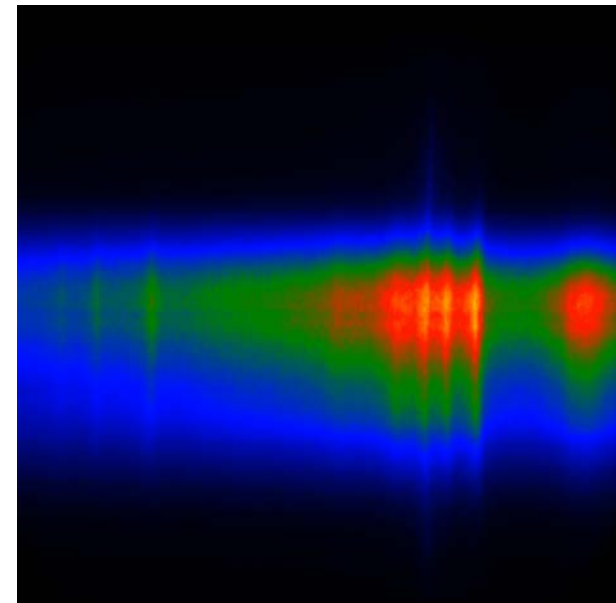
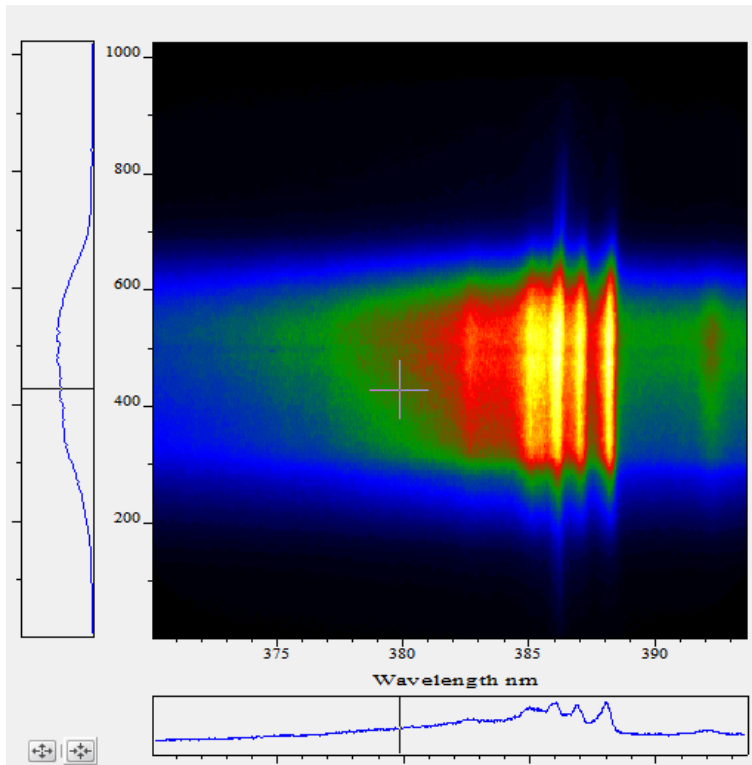
**Air, 1 atm.**



# CN Molecular Spectra, contd.

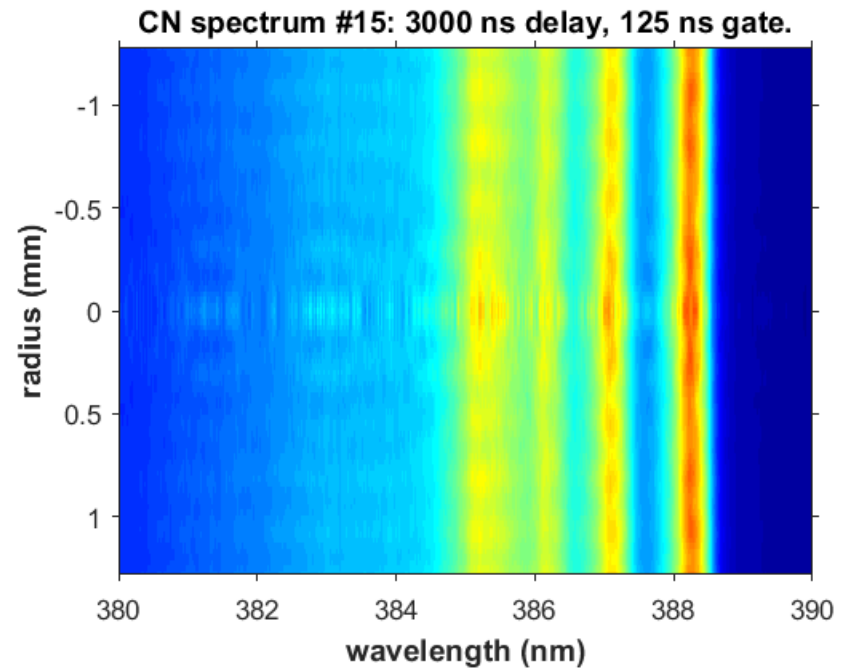
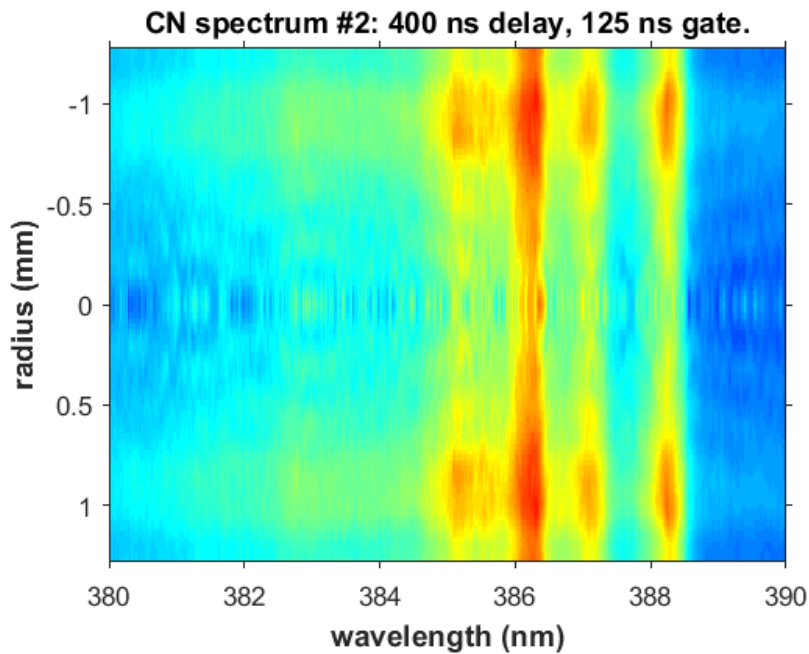
Laser-induced optical breakdown in 1:1 CO<sub>2</sub>:N<sub>2</sub> gas mixture.  
Raw spectrum: 400 ns time delay, 150mJ, 6 ns.

200 ns start, 200 ns steps



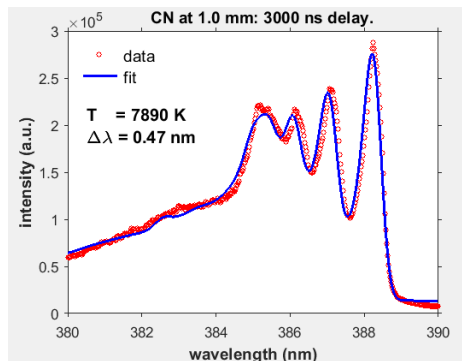
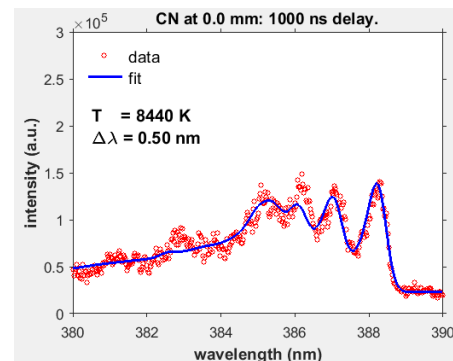
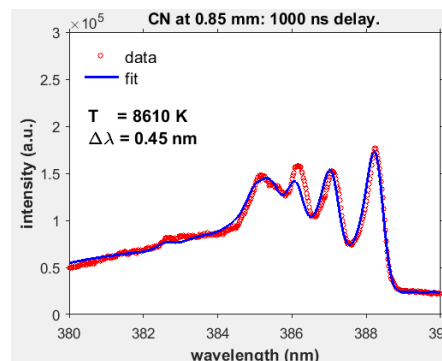
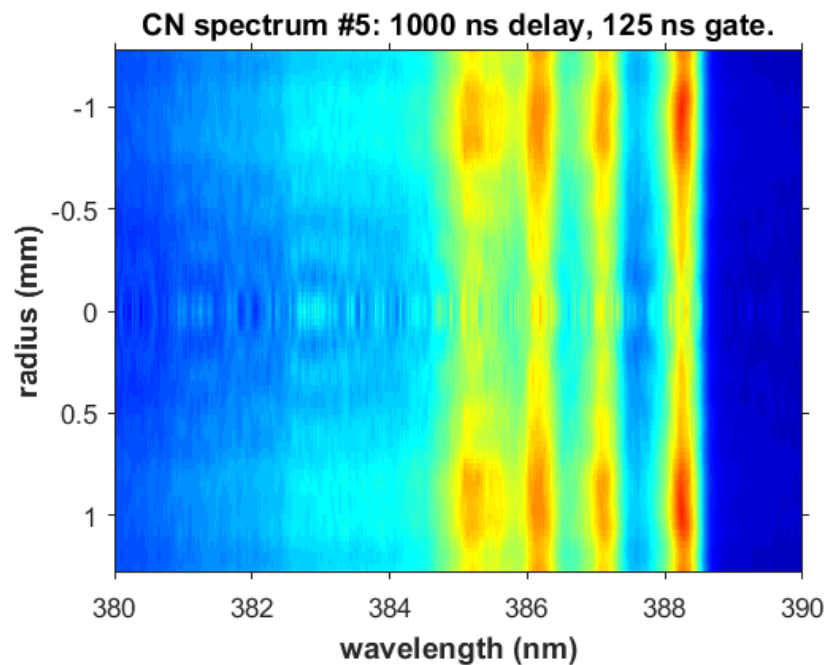
# Abel-inverted CN spectra

Laser induced breakdown in 1:1 CO<sub>2</sub>:N<sub>2</sub>



# Abel-inverted CN spectra, contd.

Laser induced breakdown in 1:1 CO<sub>2</sub>:N<sub>2</sub>



# Superposition spectra: H $\beta$ and C $_2$

## Atomic and molecular spectroscopy

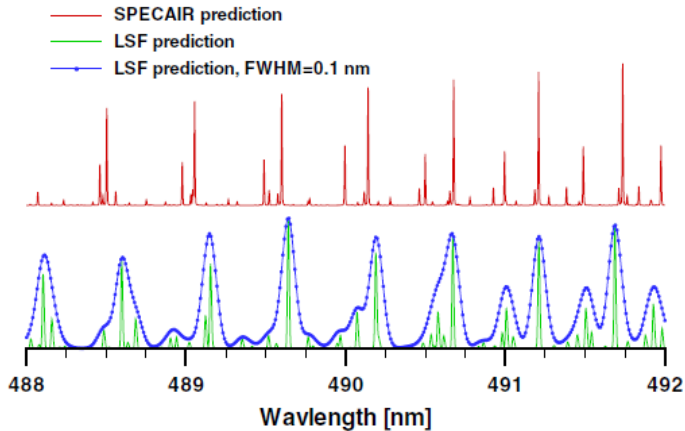


Fig. 4. (Color online) Line positions computed using SPECAIR (top) and line-strength files (LSFs) for C $_2$  (bottom) for an equilibrium temperature of  $T = 5000$  K. The broadened profile (bottom) is computed for  $\text{FWHM} = 0.1$  nm.

## Analysis of time-resolved superposed atomic hydrogen Balmer lines and molecular diatomic carbon spectra

Christian G. Parigger,<sup>1,\*</sup> Alexander Woods,<sup>1</sup> and James O. Hornkohl<sup>2</sup>

1 March 2012 / Vol. 51, No. 7 / APPLIED OPTICS B1

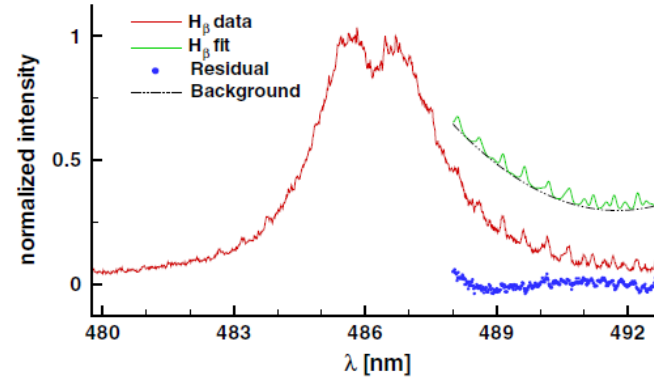


Fig. 5. (Color online) Measured H $\beta$  and fitted C $_2$  Swan band emissions.  $\Delta\tau = 2.0 \mu\text{s}$ ,  $p = 2.7 \times 10^5$  Pa. Fitted molecular emission temperature,  $0.56 \times 10^4$  K; electron excitation temperature,  $1.3 \times 10^4$  K.

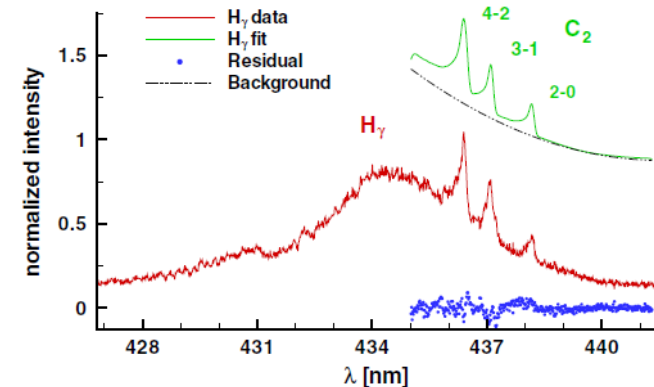
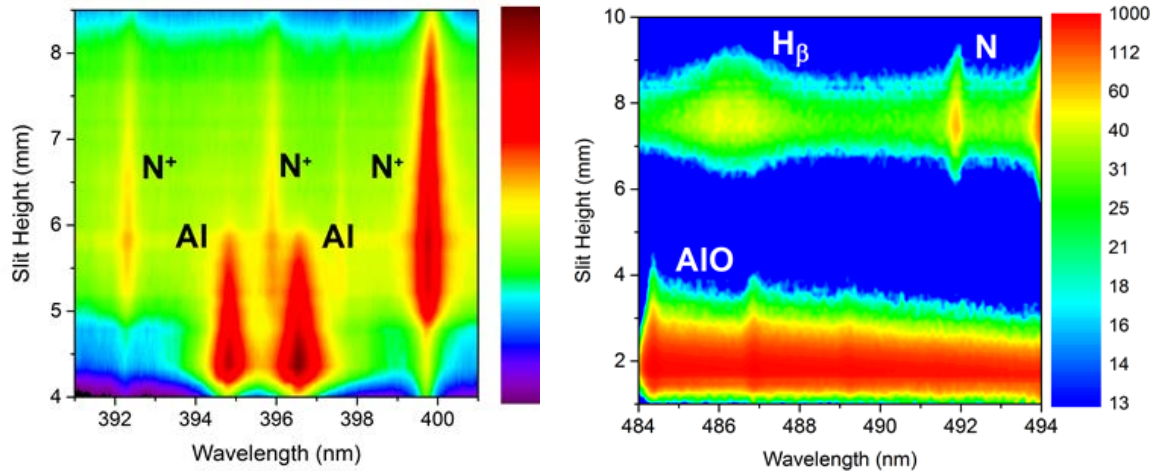


Fig. 8. (Color online) Measured H $\gamma$  and C $_2$  Swan band emissions,  $\Delta\tau = 2.0 \mu\text{s}$ ,  $p = 6.5 \times 10^5$  Pa. Fitted molecular emission temperature,  $0.48 \times 10^4$  K; electron excitation temperature,  $1.3 \times 10^4$  K.

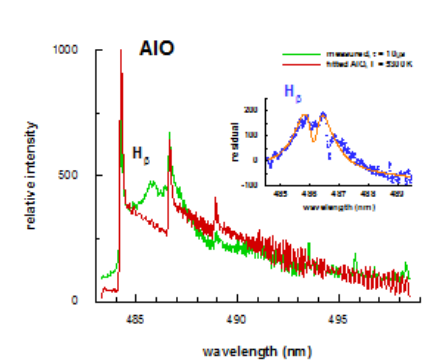
# Superposition spectra: AlO and H $\beta$

## Laser ablation in air

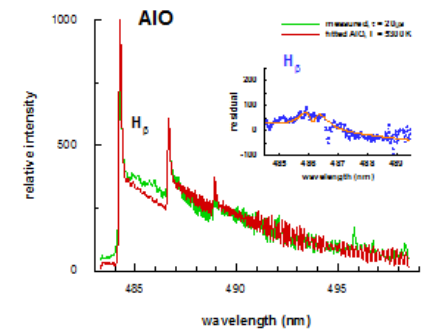


ICCD images of air and aluminium laser breakdown for 0.3  $\mu\text{s}$  (Left) and 10  $\mu\text{s}$  (Right) time delays

David Surmick, AIO, 2016, PhD University of Tennessee.  
Ghaneshwar Gautam, H, 2017, PhD, University of Tennessee.



10  $\mu\text{s}$ ,  $N_e = 0.24 \times 10^{17} \text{ cm}^{-3}$

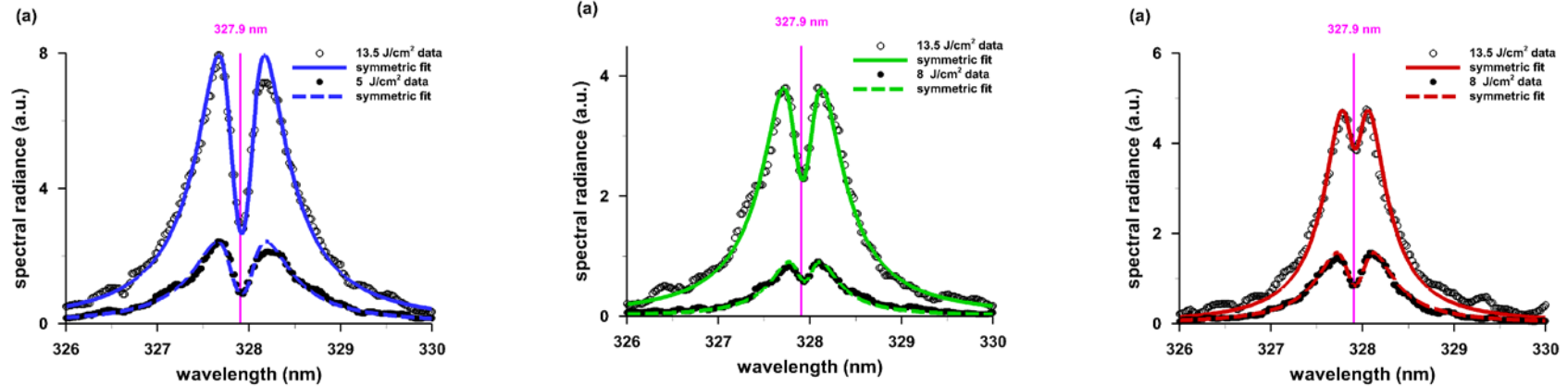


20  $\mu\text{s}$ ,  $N_e = 0.14 \times 10^{17} \text{ cm}^{-3}$

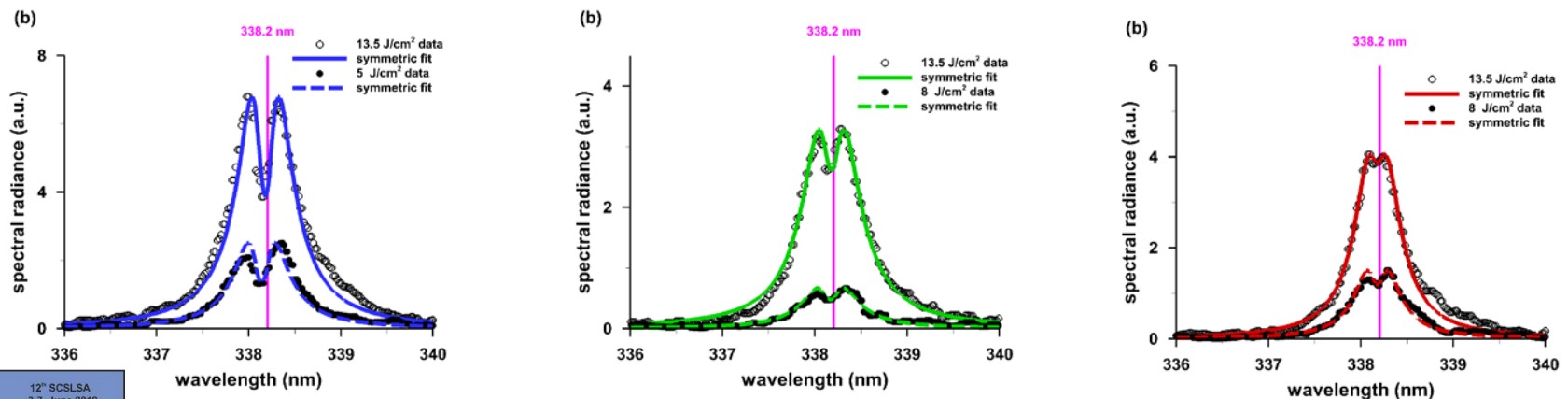


# Nano-particle plasma

## 100 nm Ag particles, collaboration with Cairo University



Self-reversal of Ag I (top) 327.9 nm, and (bottom) 338.2 nm. Laser wavelengths: 355 nm, 532 nm, and 1064 nm. Fluence of 13.5 and 8 J/cm<sup>2</sup>.



# Conclusions

- Atomic and molecular emission spectra of the type encountered in laser-induced breakdown spectroscopy occur in astrophysical spectra from white dwarf stars;
- Gas-dynamic expansion affects distribution of the laser plasma, including distributions in the kernel and just inside the expanding shock wave;
- Measured hydrogen electron densities and temperatures in the range of 1 to  $100 \times 10^{17} \text{ cm}^{-3}$  and 10 kK to 120 kK (1 to 10 eV), respectively;
- Abel-inverted hydrogen (H) and cyanide (CN) spectra indicate effects of expansion dynamics, e.g., outgoing electron density and temperature wave;
- Superposition spectra of hydrogen (H) and Swan ( $\text{C}_2$ ) bands, and H and AlO, but really would need spatial and temporal resolution;
- Self-reversal and self-absorption can be an issue for nanomaterial LIBS.

